

Exploring the trifluoromenadione core as a template to design antimalarial redox-active agents interacting with glutathione reductase†

Don Antoine Lanfranchi,^a Didier Belorgey,^a Tobias Müller,^b Hervé Vezin,^c Michael Lanzer^d and Elisabeth Davioud-Charvet^{*a,b}

Received 31st January 2012, Accepted 17th April 2012

DOI: 10.1039/c2ob25229e

Menadione is the 2-methyl-1,4-naphthoquinone core used to design potent antimalarial redox-cyclers to affect the redox equilibrium of *Plasmodium*-infected red blood cells. Exploring the reactivity of fluoromethyl-1,4-naphthoquinones, in particular trifluoromenadione, under quasi-physiological conditions in NADPH-dependent glutathione reductase reactions, is discussed in terms of chemical synthesis, electrochemistry, enzyme kinetics, and antimalarial activities. Multitarget-directed drug discovery is an emerging approach to the design of new antimalarial drugs. Combining in one single 1,4-naphthoquinone molecule, the trifluoromenadione core with the alkyl chain at C-3 of the known antimalarial drug atovaquone, revealed a mechanism for CF₃ as a leaving group. The resulting trifluoromethyl derivative **5** showed a potent antimalarial activity *per se* against malarial parasites in culture.

Introduction

One of the most dangerous infectious diseases and major health problems in the world is malaria, which affects 200–500 million people each year. The symptoms of the disease develop when the malarial parasite *Plasmodium falciparum* multiplies in human erythrocytes; therefore, most of the available drugs are directed against this stage of the parasitic cycle. Due to increasing resistance of the parasite strains against standard drugs used in medicine for more than 50 years, new treatments or drug combinations are urgently required. Indeed, many plasmodia isolates in various areas showed resistance to mainstream therapies. Drug resistance accounting for treatment failure developed not only towards the old 4-aminoquinolines like chloroquine, but also to other chemical classes such as the 1,4-naphthoquinone atovaquone **1**,¹ or more recently, to the Chinese plant-derived

artemisinins.² However, this parasite adaptation can be reversed, sometimes completely, by drug combinations of known antimalarial agents blocking two pathways in synergy; the association atovaquone **1** and proguanil (marketed as Malarone[®]) is one successful example. In this case, atovaquone **1** acts as an inhibitor of the mitochondrial cytochrome *bc1* complex³ whereas proguanil acts as a type-II antifolate; both key pathways are targeted in one single formulation. This strategy belongs to “polypharmacology”⁴ and clearly offers advantages in the fight against infectious diseases. However, combining drugs may cause unwanted drug interactions or has the drawback for pharmaceutical companies of multiplying the costly pharmacokinetic and clinical studies. The dual drug concept has been applied with some success in the search for new antimalarial agents,⁵ bringing in one single hybrid molecule the way to target several essential and synergistic pathways expressed in the parasite. By this approach two teams independently discovered dual drugs, *i.e.* hybrid molecules, acting on different pathways, interfering both with hemozoin polymerization and the redox equilibrium.^{5a,d} However, despite excellent antimalarial activities against parasites in cultures,^{5a–c} the first generation of dual drugs suffered from poor drug-like properties. This is due to their high molecular weight resulting from the attachment of two chemical entities. Therefore, our “multi-target-directed ligand design”⁶ approach was to find a common chemical structure of molecules known to exert their antimalarial action at different levels in the parasite.

Atovaquone **1** (Fig. 1) is a 2-hydroxy-1,4-naphthoquinone derivative that disturbs the electron-transport chain in the mitochondria of erythrocytic stages of *Plasmodium* parasites. The active mitochondrial electron transport chain is an important target as it regenerates the ubiquinone required as the electron

^aEuropean School of Chemistry, Polymers and Materials (ECPM) University of Strasbourg, UMR CNRS 7509, 25 Rue Becquerel, F-67087 Strasbourg, France. E-mail: elisabeth.davioud@unistra.fr; Fax: +33 (0)3 68 85 27 42; Tel: +33 (0)3 68 85 26 20

^bBiochemie-Zentrum der Universität Heidelberg, Im Neuenheimer Feld 328, D-69120 Heidelberg, Germany

^cUniversité des Sciences et Technologies de Lille, F-59655 Villeneuve d'Ascq, France

^dDepartment of Infectiology, University of Heidelberg, Im Neuenheimer Feld 324, D-69120 Heidelberg, Germany

† Electronic supplementary information (ESI) available: Characterization of redox potentials derived from cyclic voltammograms of menadione **2**, its analogues **3**, **6**, **7**, and **15**, and methylene blue (MB) as reference; cyclic voltammetry of 1 mM 2-*tert*-butyl-1,4-naphthoquinone **15** and fluoromenadione **6**; LC-MS traces showing the formation of lawsone **4** from trifluoromenadione **3** at pH 7.0; ¹H and ¹³C NMR spectra of compounds **3**, **5**, **8**, and **12**. See DOI: 10.1039/c2ob25229e

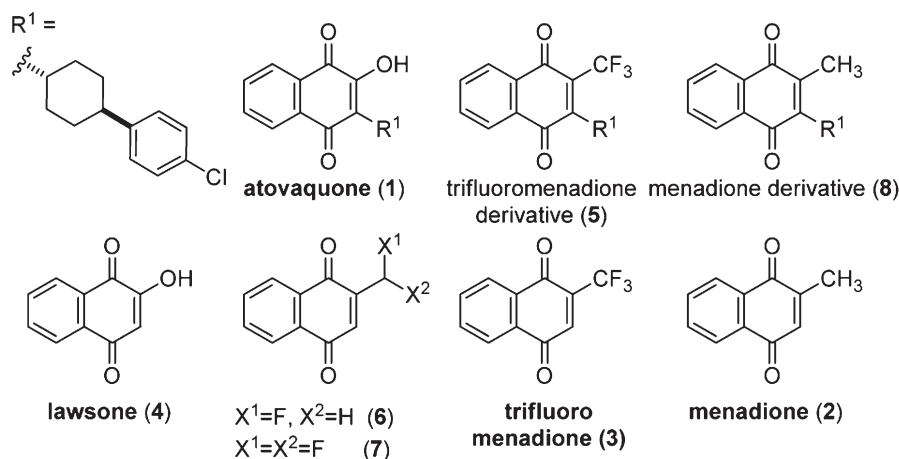
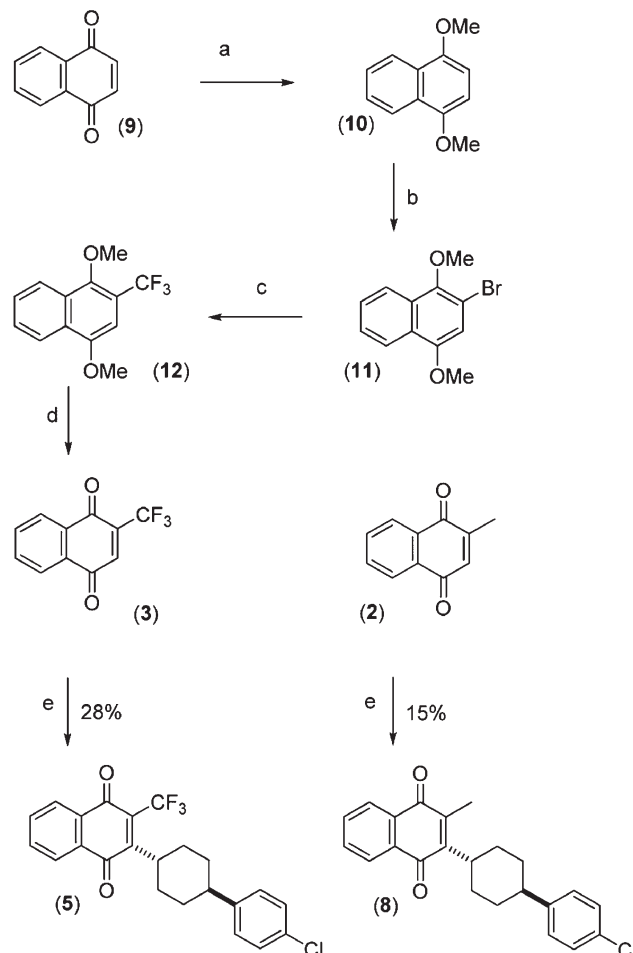


Fig. 1 Fluoromethyl and methyl analogues of menadione, lawsone and atovaquone.

acceptor for dihydroorotate dehydrogenase, an essential enzyme for pyrimidine biosynthesis. Menadione **2** and its analogues possess a 2-methyl-1,4-naphthoquinone core and are substrates of both human and *P. falciparum* glutathione reductases (*hGR* and *PfGR*, respectively).^{5a,7} and references cited therein These enzymes are known to be validated drug targets in the design of antimalarial drugs.^{5a,7,8}

During its intraerythrocytic life cycle the parasite is exposed to high fluxes of reactive oxygen species (ROS) released from heme and decomposition products generated in the course of the major hemoglobin digestion process. Therefore, the parasite survival in the host is highly dependent on an effective thiol-based redox network in *Plasmodium*-infected red blood cells. The most important protection system is the homodimeric flavoenzyme glutathione reductase (GR). *P. falciparum* glutathione reductase reduces glutathione disulfide (GSSG) into its thiol form glutathione (GSH) at the expense of NADPH. Several drugs (e.g. isoalloxazines, methylene blue, peroxynitrite, redox-active 1,4-naphthoquinones) target this enzyme.⁸

As part of our current research program including the synthesis of a variety of 1,4-naphthoquinone derivatives, we synthesized some fluoro-analogues of menadione **2** (2-methyl-1,4-naphthoquinone) and atovaquone **1**. The most striking observation was that the 2-trifluoromethyl-1,4-naphthoquinone core **3** (trifluoromenadione) showed interesting chemical reactivity that has inspired detailed investigations on this series of compounds. In particular, evidence of generation of lawsone **4** (2-hydroxy-1,4-naphthoquinone) through a vinylogous haloform reaction from the trifluoromenadione **3** let us anticipate a prodrug effect which could be applied to the formation of atovaquone from its trifluoromethyl analogue **5** *in vivo*. Therefore, the hybrid character of the final trifluoro derivative **5** was aimed at targeting different biological pathways of the parasite, *i.e.* the mitochondrial electron transport chain for pyrimidine biosynthesis and the redox equilibrium. As a successful example, introduction of a CF₃ group at C-10 of artemisinin and derivatives clearly increased the antimalarial activity of the parent drugs.⁹ In this paper we present the chemical synthesis of fluoro menadione, in particular trifluoromenadione and derivatives bearing the atovaquone alkyl chain (Scheme 1), and their



Scheme 1 Preparation of the trifluoromethyl and methyl analogues of atovaquone. *Reagents and conditions:* (a) SnCl₂ (2.5 eq.), HCl (37%), EtOH, 10 min, RT; then (CH₃O)₂SO₂ (3.0 eq.), KOH (5.0 eq.) in MeOH, acetone, 2.5 h, 60 °C (93%); (b) Br₂ (1.0 eq.), CHCl₃, 45 min, 0 °C (95%); (c) CF₃COONa (3.0 eq.), CuI (2.0 eq.), DMA–toluene, 18 h, 145 °C (49%) (d) CAN (3.0 eq.), CH₃CN–H₂O, 15 min, RT (93%); (e) AgNO₃ (0.1 eq.), (NH₄)₂S₂O₈ (1.3 eq.), (±)-*trans*-(4-chlorophenyl)cyclohexane carboxylic acid (2.0 eq.), CH₃CN–water, 2 h, 85 °C.

inhibition properties against *hGR* and *PfGR*, as well as some biological data against the multi-resistant *P. falciparum* strain Dd2.

Results and discussion

Chemistry

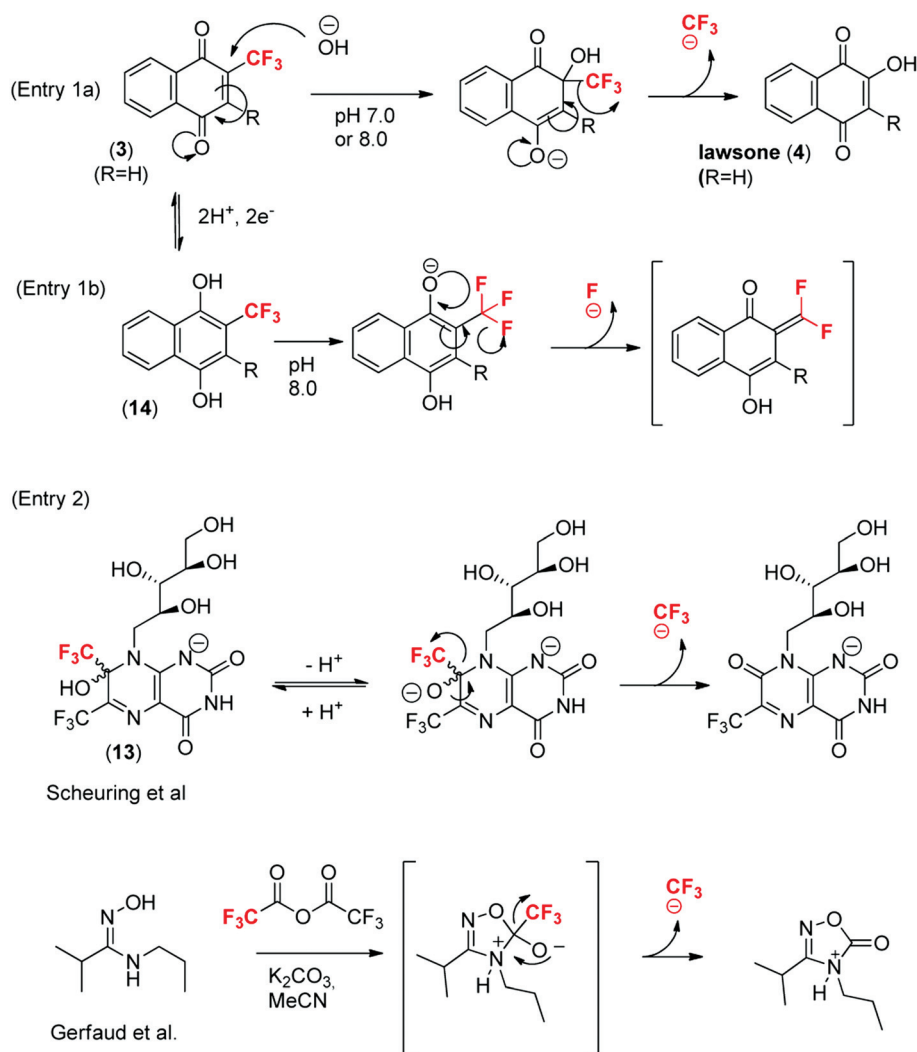
Synthesis of 2-fluoromethyl-naphthoquinone **6** and 2-difluoromethyl-naphthoquinone **7** were performed according to procedures previously described.^{7,10} Synthesis of the related trifluoro compound **3** followed a different route.

For the introduction of the trifluoromethyl group we used the method developed by Hünig and collaborators.¹¹ The mechanism is based on the *ipso* substitution of the bromine by a trifluoroacetic cuprate generated *in situ* in the reaction from CuI and sodium trifluoroacetate. With this method it was essential to remove traces of water by repeated azeotropic distillation of toluene–water out of the reaction mixture.^{5b} DMF–toluene as a solvent mixture¹² was less efficient than *N,N*-dimethylacetamide (DMA)–toluene as reported in the original paper. This is most likely due to the lower inside temperature and therefore to longer

reaction times. However, prolongation of the reaction time to more than 18 h did not improve the yield, probably because of the instability of the trifluoroacetic cuprate. In our experiments a reaction temperature between 140 and 150 °C was optimal. Menadione and trifluoromenadione derivatives **5** and **8**, bearing the atovaquone side-chain, were synthesized *via* the known silver catalyzed decarboxylation reaction¹³ from the starting menadione **2** and trifluoromenadione **3**, respectively, according to Scheme 1. In both cases, the yields of the reaction were poor (15% and 28%) due to a difficult purification step and to the instability of the fluoro product on silica gel, respectively.

Postulated chemical reactivity and haloform reaction

The structural features of trifluoromenadione **3** let one assume that this compound might undergo a vinylogous haloform reaction (Scheme 2, entry 1a). Although the trifluoromethyl carbanion is a poor nucleofuge, Scheuring *et al.*¹⁴ observed that a lumazine derivative **13** decomposed under neutral or mild basic conditions by elimination of a CF₃ group (Scheme 2, entry 2). Very recently, Gerfaud *et al.*¹⁵ prepared 1,2,4-oxadiazol-5-ones



Scheme 2 Vinylogous haloform or trifluoromethyl elimination reactions and related mechanisms to eliminate a trifluoromethyl group.

from amidoximes with trifluoromethyl anion acting as a leaving group (Scheme 2, entry 2). In our case, HPLC analysis confirmed that the trifluoromethyl group of **3** in conjugation to the Michael system can undergo the last step of the haloform reaction under neutral (pH 7.0) and basic conditions (pH 8.0) ending up with 2-hydroxy-1,4-naphthoquinone **4** (lawsone) (see paragraph describing the chemical stability of trifluoromenadione **3** versus its derivative with atovaquone side-chain **5**). Another possible reactivity of the trifluoromenadione core relies on its ability to be reduced into its hydroquinone counterpart **14** (Scheme 2, entry 1b). Indeed, it is well documented that 2- and 4-trifluoromethylphenols can undergo fluorine elimination to release the quinone methide.¹⁶ Therefore, we anticipated that under physiological conditions nucleophiles (thiols...) would attack the Michael system of the trifluoromethyl derivatives, releasing fluorine and leaving the nucleophile attached to the 1,4-naphthoquinone moiety. The behavior of trifluoromenadione **3** was also studied both by electrochemistry and in NADPH-dependent glutathione reductase-catalyzed reactions, and analyzed by mass spectrometry. Its C-3 alkylated derivative **5** has different structural features compared to the lumazine derivative of Scheuring *et al.*,¹⁴ but it supports our finding that in principle the CF₃ group can be regarded as a leaving group under certain conditions. Thus, by combining the properties of trifluoromenadione **3** as a putative redox-active mechanism-based GR inhibitor with atovaquone **1**-related inhibitory capabilities of the respiratory chain of the parasite,^{3,17} we synthesized its hybrid derivative **5** which might be – in principle – regarded as a prodrug of atovaquone **1** targeting both the reducing milieu *per se* and the respiratory chain after the loss of the CF₃ group.

Electrochemical reduction of substituted menadione derivatives

The redox potential values of the non fluoro- and the fluoro-naphthoquinones were determined by cyclic voltammetry in order to study the influence of the fluorine atom on the π - π electron acceptor properties (Fig. 2, and Table S1† in ESI†). The relative electrochemical behavior of the naphthoquinones was investigated in CH₂Cl₂ for reasons of better solubility and compared with the parent menadione **2**, and also with the known redox-cycler methylene blue (Table S1†). The cyclic voltammograms of the synthesized naphthoquinones in CH₂Cl₂ showed two reduction- and two to three oxidation-waves (Panels A–C, Fig. 2). The midpoint potentials were determined as E°_1 and E°_2 values for the formation of the semiquinone anion (NQ^{•-}) and the dianion (NQ²⁻), respectively (Table S1†). The half-wave potentials $E^\circ = (E_{pc} + E_{pa})/2$ is defined as the average of the anodic (E_{pa}) and cathodic (E_{pc}) peak potentials. The redox potentials of menadione were measured as reference. For menadione the redox reactions are kinetically reversible in the cyclic voltammogram (Fig. 2, panel A), and the E°_1 and E°_2 values can be identified as thermodynamic values. This is evidenced by the ratio I_{pc}/I_{pa} of 0.93, a value close to 1. The electrochemical behavior of the trifluoromenadione **3** is also very similar in reversibility as judged from the cyclic voltammogram (Fig. 2, panel B) and the I_{pc}/I_{pa} ratio of 0.96 in both one- and two-electron reduction waves. However, the presence of the trifluoromethyl group led to an important shift in both 1e- and 2e- reduction

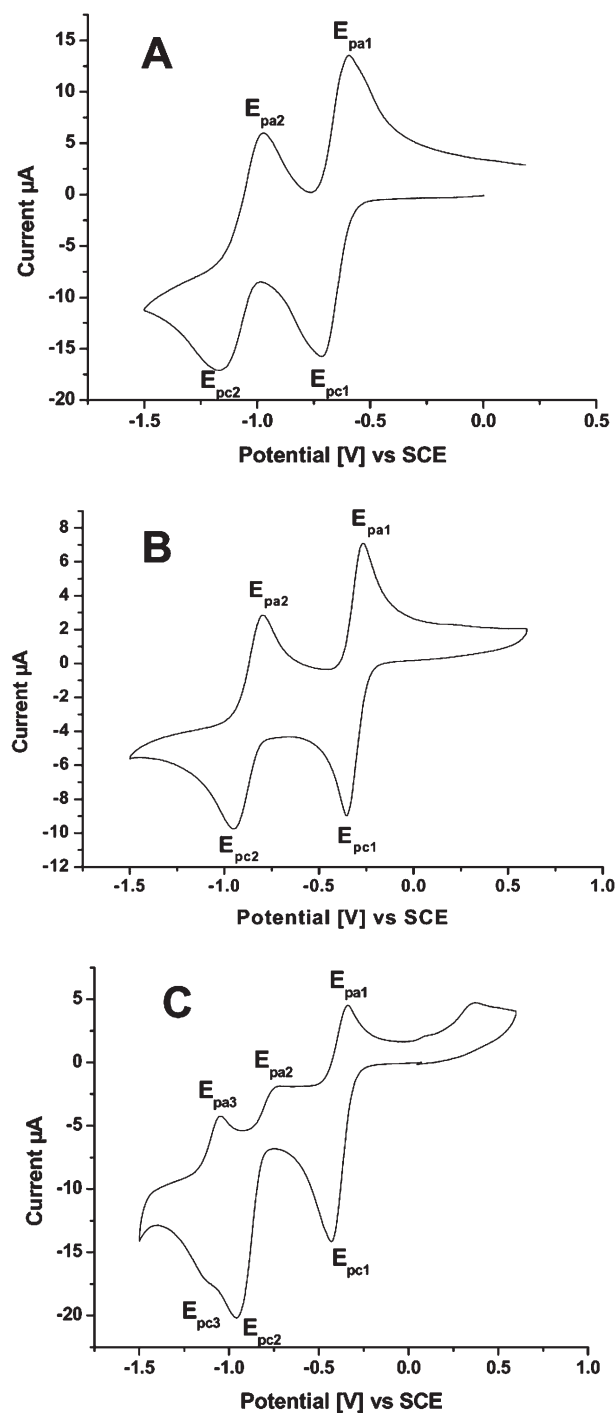


Fig. 2 Cyclic voltammograms of menadione **2** (panel A), and of its fluoromethyl-1,4-naphthoquinone analogues **3** (panel B, CF₃) and **7** (panel C, CHF₂) recorded at platinum electrode in CH₂Cl₂ with 0.1 M Bu₄NBF₄ as supporting electrolyte at 0.2 V s⁻¹ scan rate.

potentials (E°_1 and E°_2) values (Table S1†) revealing the strong oxidant character of the molecule.

By contrast, 2-*tert*-butyl-1,4-naphthoquinone **15** (Fig. S1,† panel A, in ESI) – which also showed quasi-reversible one- and two-electron transfer reactions with I_{pc}/I_{pa} ratio of 0.94 and 0.96, respectively – is characterized by a shift of both E°_1 and E°_2 to

more negative values. In the case of the monofluoromethyl-menadione **6** (Fig. S1,† panel B, in ESI) and the difluoromethyl-menadione **7** (Fig. 2, panel C), the I_{pc}/I_{pa} ratio of 0.36 and 0.12 in two electron reduction reactions, respectively, indicate that the dianion forms are not completely stable. The formation of the quinone methide species followed by polymerization might be responsible for the non-reversibility of the electron transfer reactions in agreement with earlier literature observations.^{10,11,18} The presence of a marked third wave of oxidation in the cyclic voltammogram of **7** supports the hypothesis of quinone methide polymerization. As for trifluoromenadione **3** ($E^\circ_1 = -0.308$ V/standard calomel electrode (SCE)), one-electron reduction of **7** also occurs with more positive potential values than those observed for menadione **2** ($E^\circ_1 = -0.385$ V/SCE versus $E^\circ_1 = -0.65$ V/SCE for menadione **2**), rendering both fluoro analogues of menadione **7** and **3** potential effective substrates of both glutathione reductases.

Inhibition of *P. falciparum* and human glutathione reductase under steady-state conditions

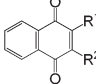
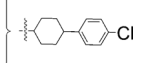
The IC_{50} values of menadione **2**, its fluoro-analogues **3**, **6**, **7**, atovaquone **1** and its derivatives, **5** and **8**, were evaluated under steady-state conditions using a concentration of 1 mM GSSG in the assay. Such a high GSSG concentration does not represent cell physiological conditions but a concentration that is toxic for the parasite. In the past, several inhibitors were identified as potent *hGR* and *PfGR* inhibitors with inhibition constants K_i values in the low micromolar range: methylene blue is a non-competitive inhibitor,¹⁹ while menadione **2** is a reversible uncompetitive inhibitor with respect to NADPH and to GSSG. Both redox-active agents behave as subversive substrates of the *Plasmodium* enzyme in NADPH reactions in the absence of GSSG.²⁰

We used menadione **2** as a reference to compare the inhibition properties of fluoro-menadione analogues in the *hGR* and *PfGR* assays. Menadione **2** displayed IC_{50} values of 27.5 μ M and 42.0 μ M (Table 1) against *hGR* and *PfGR*, respectively. All fluoro-analogues showed lower IC_{50} values than those of menadione **2**. Trifluoromenadione **3** was the most potent inhibitor with IC_{50} values of 4.3 μ M and 7.0 μ M for *hGR* and *PfGR*, respectively. The analogues of atovaquone **5** and **8** displayed lower inhibitory capabilities below 25 μ M. Determination of exact IC_{50} values in these enzymic assays was not possible due to the precipitation of the compounds in solution at concentrations higher than 25 μ M.

Human glutathione reductase-catalysed reduction

The ability of *hGR* to reduce the fluoro menadione analogues was studied by following the oxidation of NADPH in the presence of increasing naphthoquinone concentrations and compared to the intrinsic NADPH oxidation activity of the enzyme in the absence of naphthoquinone (NQ) in open air. When NADPH consumption was followed, **7** was reduced by *hGR* with a catalytic efficiency, expressed by the k_{cat}/K_m value, 20-fold higher than the values determined for menadione **2** (Table 2), mainly due to a better rate of turnover, 42-fold higher than for menadione **2**. In contrast, the catalytic efficiency of **3** was only 1.3-fold higher

Table 1 IC_{50} values^a of fluoromethyl analogues of menadione as inhibitors of human and *Plasmodium falciparum* glutathione reductases under steady-state conditions

	R ¹	R ²	IC_{50} (μ M) <i>hGR</i> assay ^a	IC_{50} (μ M) <i>PfGR</i> assay ^a
Menadione 2 ^b	–CH ₃	–H	27.5	42.0
6 ^c	–CH ₂ F	–H	5.4	27.5
7 ^c	–CHF ₂	–H	20.0 ^d	22.8 ^d
3 ^c	–CF ₃	–H	4.3	7.0
Lawsone 4 ^e	–OH	–H	>100	>100
5 ^e	–CF ₃		>25	>25
8 ^e	–CH ₃		>25	>25
Atovaquone 1 ^e	–OH		>25	>25

^a In the presence of 1 mM GSSG and 100 μ M NADPH, 1% DMSO.

^b From ref. 10. ^c Not corrected for NADPH oxidase activity. ^d From ref. 7. ^e Precipitation of the compound precluded determination of the IC_{50} value.

Table 2 Human glutathione reductase-catalysed quinone reduction^a

Compounds	K_m (μ M)	k_{cat} (s ^{–1})	k_{cat}/K_m (mM ^{–1} s ^{–1})
Menadione 2 ^b	31.2	0.16	5.1
7 (CHF ₂) ^c	66.2	6.70	101.4
3 (CF ₃)	155.5	1.05	6.8

^a For GSSG as a substrate of *hGR* from ref. 19: $K_m = 65$ μ M, $k_{cat} = 210$ s^{–1}, $k_{cat}/K_m = 3231$ mM^{–1} s^{–1}; as a substrate of *PfGR*: $K_m = 83$ μ M, $k_{cat} = 165$ s^{–1}, $k_{cat}/K_m = 1988$ mM^{–1} s^{–1}. ^b From ref. 7. ^c From ref. 20a.

than that for menadione **2**. No NADPH consumption was observed when atovaquone **1** or its analogues **5** and **8** were used as a substrate at concentration of up to 25 μ M or lawsone **4** at concentration of up to 100 μ M in both *hGR* and *PfGR* assays. At higher concentration precipitation of those two atovaquone analogues **5** and **8** occurred.

Time-dependent inactivation of glutathione reductases by fluoromethyl analogues of menadione

Time-dependent inhibition of *hGR*s was studied using the GSSG reduction assay to evaluate the residual activity of reacted enzymes. Upon incubation with NADPH and the substrates, inactivation of *hGR* by **3** and **7** followed pseudo-first order reaction kinetics. The experimental data allowed the application of the derivation by Kitz and Wilson²¹ for irreversible inactivation. A semi-logarithmic plot of the fraction of non-inhibited enzyme activity $\ln(v_i/v_0)$ versus incubation time yielded straight lines with increasing slopes at short time periods, equivalent to the apparent rate constant of irreversible inhibition (k_{obs}). The secondary plot expressing k_{obs} as a function of inhibitor concentration followed eqn (1):

$$k_{obs} = (k_i \times [I]) / (K_I + [I]) \quad (1)$$

where K_I is the dissociation constant of the inhibitor-enzyme complex and k_i is the first order rate constant for irreversible inactivation, respectively. The k_{obs} data versus **3** (or **7**) were

Table 3 Kinetic parameters of human glutathione reductase inactivation by fluoromethyl analogues of menadione

Compounds	K_I (μM)	k_i (min^{-1})	k_i/K_I ($\text{mM}^{-1} \text{s}^{-1}$)	$t_{1/2}$ (min)
7 (CHF_2) ^a	66.2	7.0	1.8	0.1
3 (CF_3)	49.5	3.4	1.1	0.2

^a From ref. 7.

fitted to eqn (1) which resulted in the determination of the dissociation constant for **3** and **7**-GR complexes and the first order rate constant for irreversible inactivation, respectively, as $K_I = 49.5 \mu\text{M}$ and $k_i = 3.4 \text{ min}^{-1}$ for **3** and $K_I = 66.2 \mu\text{M}$ and $k_i = 7.0 \text{ min}^{-1}$ for **7**, allowing estimation of a second order rate constant $k_i/K_I = 1.1 \text{ mM}^{-1} \text{ s}^{-1}$ for **3** and $k_i/K_I = 1.8 \text{ mM}^{-1} \text{ s}^{-1}$ for **7** (Table 3). The resulting half-times ($t_{1/2}$) of inactivation of *h*GR were determined as 0.2 min and 0.1 min for **3** and **7**, respectively (Table 3). We were not able to measure any kinetic constants for **5**, albeit at $25 \mu\text{M}$ *h*GR is inhibited at 65%. An approximate observed half-time of inactivation of 8.5 min can be deduced from short time of inhibition at this concentration (<5 min). This is 6.5 and 10.6 fold higher than the observed half-time calculated for **3** and **7** at $10 \mu\text{M}$ (1.3 and 0.8 min, respectively). The bulkiness of the cyclohexane chain of the hybrid molecule **5** might in part explain the less effective *h*GR inactivation by compound **5** compared to tri- and di-fluoromenadione **3** or **7**. Hence, the observed time-dependent inactivation of *h*GR by compound **5** is thought to play a role in the tests using *Plasmodium*-infected red blood cells.

Mass spectrometric analyses of *Pf*GR inactivated by di- and tri-fluoromenadiones

In order to gain a better understanding of enzyme kinetics with di- and tri-fluoro menadione derivatives we investigated the mass spectra of inactivated GR enzymes. *P. falciparum* GR solution ($15 \mu\text{M}$, 1% DMSO), was allowed to react with NADPH and **3** or **7**, in the presence of 4% DMSO final. ESI-MS spectra of dialyzed *Pf*GR solutions – either pre-reacted in the presence of $200 \mu\text{M}$ NADPH and $200 \mu\text{M}$ trifluoromenadione **3** (panel A), or alone (panel B) – were recorded under identical denaturing conditions. The enzyme alone displayed 100% residual activity while the pre-reacted mixtures with NADPH and the inhibitor (with 4% DMSO) showed a residual activity of 15% and 18%, respectively, in the standard 1 mM GSSG reduction assay.

Both *Pf*GR, unreacted and inactivated by **3** or **7** were subjected to ESI mass spectrometry analysis. Whatever the reagent (no DMSO, 4% DMSO, difluoromenadione **7**, trifluoromenadione **3**), ESI-MS analysis of *Pf*GR displayed m/z peaks revealing a protein species of 56 506 Da corresponding to the monomer along with a dimer species of 113 012 Da, evidencing “apparent absence of covalent binding” between the inhibitor and the protein (Fig. 3). However, in the presence of the inhibitor and NADPH, the mass spectrum of the reacted enzyme displayed a strong background and complete disappearance of the mass peaks of the monomer species which characterized the presence of the *Pf*GR dimer in solution. The ESI-MS spectrum did not show any mass peak of the alkylated enzyme because most of

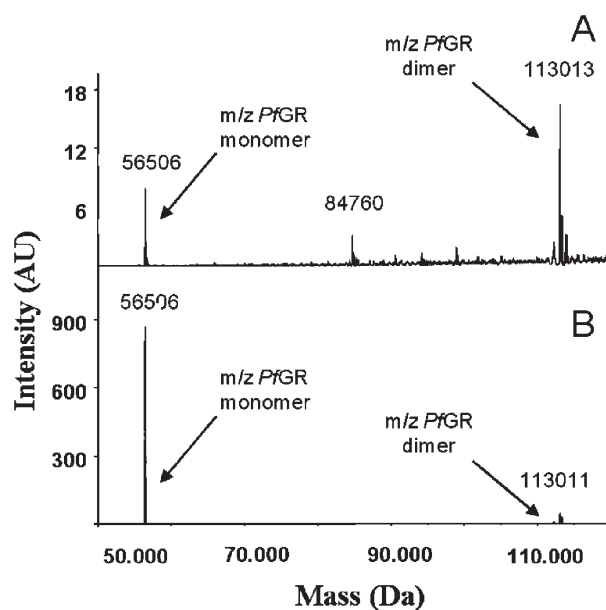
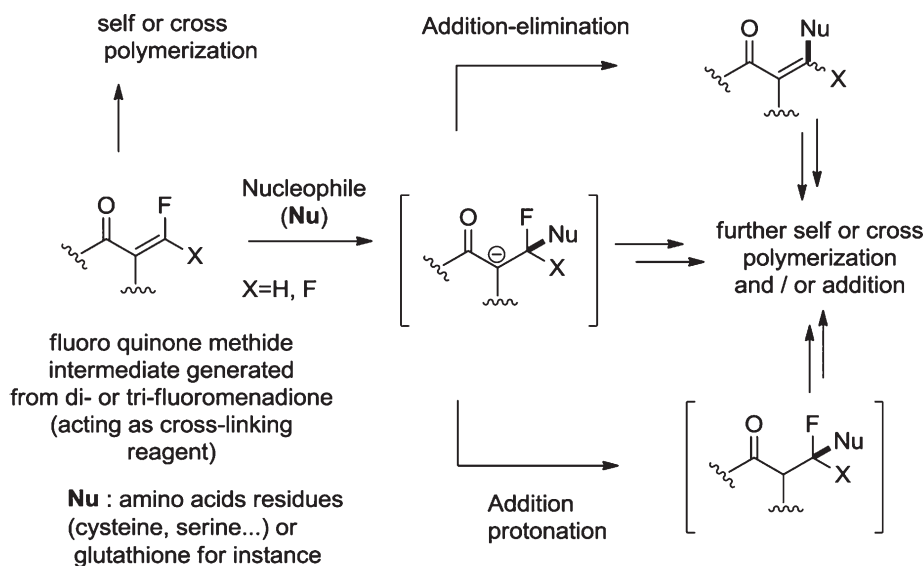


Fig. 3 ESI-MS spectra, recorded under identical denaturing conditions, of dialyzed *Pf*GR solutions ($15 \mu\text{M}$, 1% DMSO), either (panel A) pre-reacted in the presence of $200 \mu\text{M}$ NADPH and $200 \mu\text{M}$ **3**, or (panel B) not pre-reacted.

the enzyme was aggregated and little soluble protein remained in solution (see the background of the baseline). The similar phenomenon occurred with the thioredoxin-glutathione reductase from *Schistosoma mansoni* when some enzyme crystallization experiments were carried out with difluoromenadione derivatives; most of the enzyme was recovered inactivated and aggregated.²² As previously discussed,^{7,10} following reduction, the difluoromenadione core through the quinone methide is highly reactive towards nucleophiles; it acts as a difluoro acrolein very prone to polymerization (Scheme 3). The fact that the difluoromenadione **7** inhibited both *h*GR and *Pf*GR with higher IC_{50} values than the values observed for the corresponding trifluoromenadione **3** (Table 1) might be related to the fast precipitation of an inactivated insoluble **7**-reacted enzyme in the cuvette of the spectrophotometric assay upon polyalkylation or cross-linking reactions.⁷ To support this, the cross-linking capabilities of the difluoro quinone methide can be compared to the reactivity of *gem*-difluoroalkenes, which are known to be exclusively attacked by nucleophiles at the *gem*-difluoromethylene carbon atoms to form β -fluorocarbanions.²³ Further additions to the carbanions might lead to insoluble cross-linked protein (polymers). However, the elucidation of the structure of the cross-linked protein was extremely difficult due to their lack of stability and solubility.

The antiparasitic and cytotoxic activities *in vitro*

Inhibition of the growth of *P. falciparum* by the naphthoquinones was evaluated by determining the inhibitor concentration required to kill 50% of the parasite (ED_{50} values). The antimalarial activities of the fluoro analogues of menadione were tested against the



Scheme 3 Structure and reactivity of difluoro quinone methide and related β -fluorocarbanion generating further additions.

chloroquine-sensitive strain 3D7 and the chloroquine-resistant strain K1. The cytotoxicity of the compounds against human cells was determined in assays using the human nasopharyngeal carcinoma (KB) cell line to enable an estimation of the therapeutic index. This parameter is defined by the ratio of the ED_{50} value measuring the cytotoxicity against human cells over the ED_{50} value measuring the antimalarial efficacy. Menadione displayed ED_{50} values of 9.6 μ M and 12.0 μ M against 3D7 and K1, giving a therapeutic index of 3.6 and 2.9, respectively.

All fluoro analogues of menadione are more active than menadione²⁴ itself against both strains (Table 4). Only in the case of **6** the cytotoxicity was higher than menadione. Difluoromenadione **7** and trifluoromenadione **3** displayed a much more favorable therapeutic index, the compounds being 7 to 27 fold less cytotoxic than menadione. Surprisingly, **6** displayed a two-fold lower ED_{50} value toward the resistant K1 strain *versus* the sensitive 3D7 strain. Nonetheless, the therapeutic index is rather low ranging from 2.4 to 4.6. Difluoromenadione **7** displayed the lowest ED_{50} values against 3D7 and K1, as well as a low cytotoxicity with a therapeutic index of 109–132. In addition, trifluoromenadione **3** has fairly improved antiparasitic activities compared to menadione but the cytotoxicity significantly decreased (therapeutic index 114–115). The lowest cytotoxic effects of **3** in the series of the three fluoromethyl naphthoquinones, in addition to the CF_3 elimination reaction, directed the selection of the trifluoromenadione core to synthesize the potential hybrid prodrug **5** with the cyclohexyl chain of atovaquone. The atovaquone–menadione hybrid molecules **5** and **8** were tested against the Dd2 strain of *P. falciparum* which is atovaquone-sensitive but multidrug-resistant towards 4-aminoquinolines. Used as references, chloroquine and atovaquone displayed ED_{50} values of 110 ± 13 nM and 0.18 ± 0.03 nM against the Dd2 strain, respectively. The C-3-alkylated menadione derivative **8** was inactive against this strain ($ED_{50} = 1500 \pm 200$ nM). In contrast, its trifluoro derivative **5** showed potent antimalarial effects with an ED_{50} value of 20 ± 10 nM (Fig. 4).

Table 4 *In vitro* antimalarial activity and cytotoxicity against human cells of menadione derivatives and its fluoro analogues

Compounds	ED_{50} (μ M) 3D7	ED_{50} (μ M) K1	ED_{50} (μ M) KB
Chloroquine	0.005	0.550	127.3
Menadione 2 ^a	9.6	12.0	34.3
6 (CH_2F)	8.5	4.5	20.5
7 (CHF_2)	1.9	2.3	250.3
3 (CF_3)	8.0	8.1	923.0

^a From ref. 24.

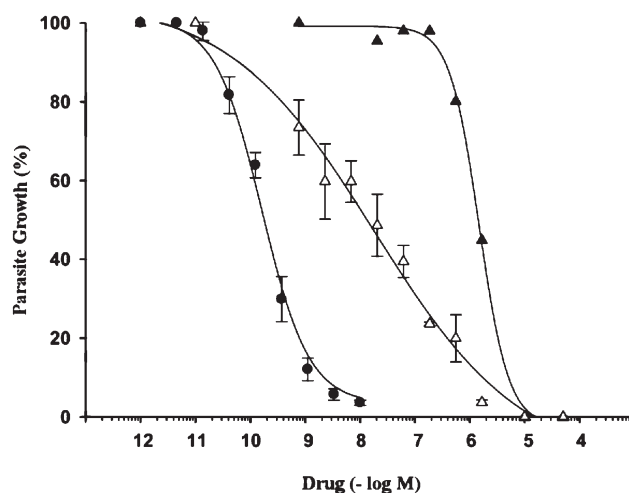


Fig. 4 Dose response curves for *in vitro* growth inhibition of malarial parasites (Dd2) by atovaquone **1** and atovaquone–menadione hybrid molecules **5** and **8**. Highly synchronized *P. falciparum* cultures were incubated with increasing concentrations of compounds and the percentage of parasite growth was determined after 72 h of drug exposure. The data point were fitted using a three parameters Hill function to calculate the ED_{50} values. (●) Atovaquone **1**, (Δ) **5**, (▲) **8**.

The chemical stability of trifluoromenadione **3** versus its C-3 alkylated analogue **5**

Menadione **2** is a known Michael acceptor. It readily reacts with glutathione at carbon 3.²⁵ In order to study the reactivity of its fluoromethyl analogues we studied the conjugation of **3** towards one equivalent of glutathione under physiological conditions. The reaction mixtures were analyzed by HPLC and positive ESI-MS spectra. Under these conditions, menadione **2** reacts by forming the related 3-glutathionyl-menadione derivative characterized by a m/z peak at 478.2. At pH 8.0, trifluoromenadione **3** (t_R of 18.72 min) disappeared as a function of time; one major product which did not correspond to its glutathione conjugate was observed with a t_R of 15.43 min and a m/z peak of 174.4. While vinylogous fluoromethyl ketones²³ and fluoromethyl-1,4-naphthoquinones^{7,10} were reported to generate highly electrophilic quinone methide upon reduction and elimination of one to three fluorine atoms, the new major metabolite of trifluoromenadione **3** did not correspond to any of the expected adduct with glutathione at the carbon 3 or at the terminal double bond of the methide following SN_2' substitution. In comparison with an external reference, the product was assigned to lawsone **4**, confirmed upon co-injection to the HPLC apparatus and ESI-MS analysis, and by LC-MS. The chemical stability of trifluoromenadione **3** and its analogue **5** alkylated at C-3 was investigated at pH 7.0 and 8.0 in quasi-physiological conditions by LC-MS analysis.

At pH 8.0, trifluoromenadione **3** was unstable and was almost instantly transformed into lawsone **4** and other minor compounds. At pH 7.0 in 5 mM ammonium acetate, the formation of lawsone **4** was also observed by LC-MS, albeit slower than at pH 8.0 (Fig. 5). After 5 h trifluoromenadione **3** was almost entirely transformed into lawsone **4** (93%) with a half-time for the reaction of ~105 min (the LC-MS traces are given in the ESI, Fig. S2†). In the same conditions (pH 7.0 and 8.0), the trifluoromenadione derivative **5**, alkylated at C-3, remained stable for up to 24 h. There was no evidence of atovaquone formation from its trifluoro derivative. From the chemical stability

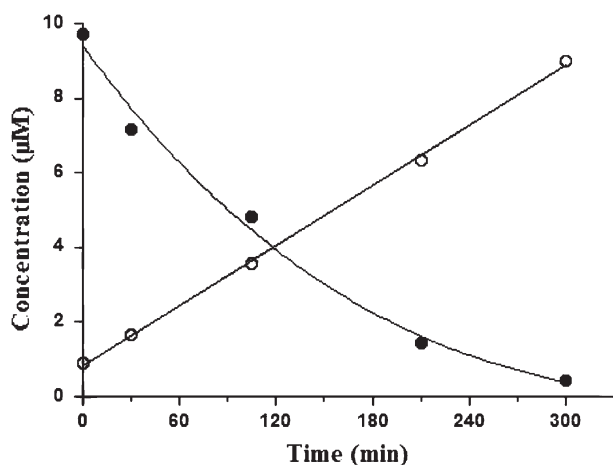


Fig. 5 Chemical stability of trifluoromenadione **3** and formation of lawsone **4** at pH 7.0. The stability of **3** (●) and the formation of lawsone **4** (○) were followed at pH 7.0 as a function of time by LC-MS and the concentration calculated from calibration curves.

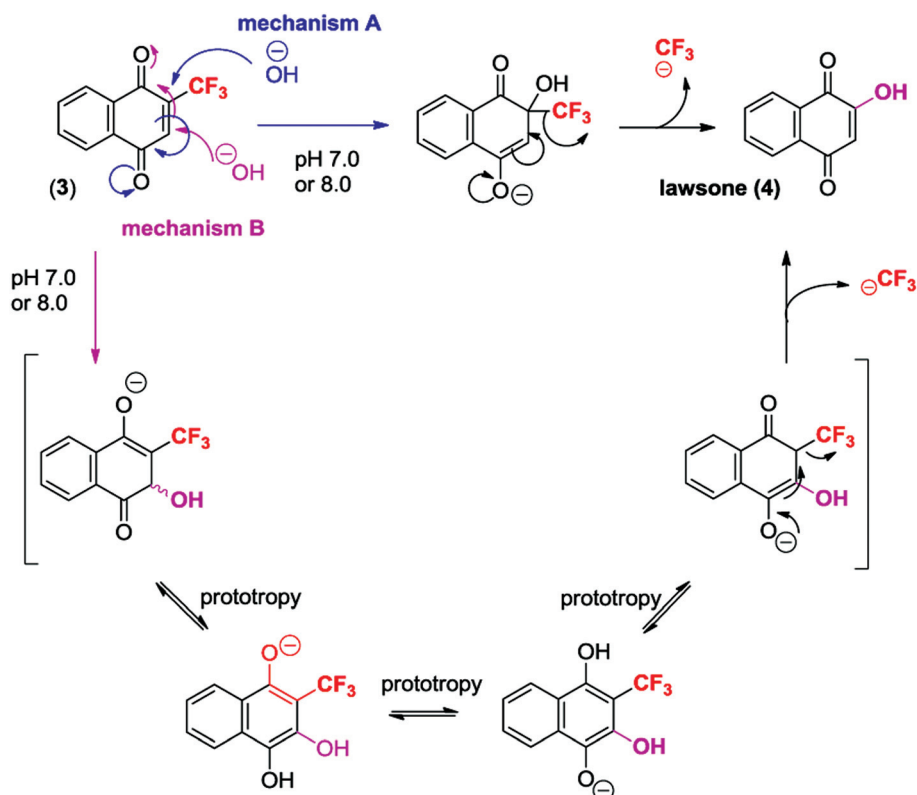
study, it is obvious that the *trans*-4-(4-chlorophenyl)cyclohexane chain prevents the CF_3 elimination from the C-3 alkylated trifluoromenadione **5**.

Hence, an alternative mechanism for CF_3 elimination from trifluoromenadione **3** and lawsone **4** generation (Scheme 4, mechanism B) was thus evidenced in contrast to the initially postulated mechanism A (Scheme 4). It is proposed to involve hydroxide attack at C-3 instead of C-2 and prototropic interconversion of structural isomers leading to the elimination of the CF_3 group.

Conclusion

Following the rationale to develop a hybrid prodrug of atovaquone by merging two entities, trifluoromenadione **3** and atovaquone **1**, in a single cleavable chemical entity, a dual effect could be expected from the release of two active principles targeting the redox equilibrium and the mitochondrial electron transport chain for pyrimidine biosynthesis, both essential pathways for the malarial parasites. The prodrug effect was based on the observed CF_3 elimination from trifluoromenadione **3** to lawsone **4** under quasi-physiological conditions. Hence, the design of the multifunctional trifluoromenadione **5** bearing the side-chain of atovaquone was attempted as a drug combination with a better potential for malaria therapy. However, despite the fact that the trifluoro derivative **5** was found not cleavable, as opposed to its lower analogue trifluoromenadione **3**, the resulting hybrid molecule can be defined as a redox-active 1,4-naphthoquinone killing the parasites *per se*, with other pharmacological effects in addition to their mechanism-based inhibition towards GR. The *trans*-4-(4-chlorophenyl)cyclohexane chain is proposed to be the motif recognized by a transporter protein conferring long plasma half-life to atovaquone **1** in humans, as recently shown.²⁶ Therefore, it might be possible that the hybrid trifluoromenadione **5** bearing the atovaquone side-chain is transported in a similar way, but its structural features might allow an alternative pathway, by depletion of certain nucleophiles present in infected red blood cells, as evidenced here for glutathione reductase inactivation. Many electrophilic moieties were characterized as frequent hits or assay-interfering compounds because they interact with a broad panel of thiol targets, rendering them practically useless in drug discovery. Therefore, numerous modern strategies proposed to employ these moieties attached to “privileged scaffolds” known to be selectively uptaken by the target pathogen transporters. Considering both opinions, the positive perspective of our polypharmacological approach in antimalarial drug discovery results from combining these “privileged active principles” acting on various targets, in one fused molecule which can be regarded as a new potent antimalarial redox-active agent to further optimize.

Besides the study on the reactivity of trifluoromenadione, the present investigations have provided key information on time-dependent GR inactivation by fluoro menadiones. Furthermore, our data shed light on the distinct mode of interaction of 1,4-naphthoquinones with human and *P. falciparum* GRs: in contrast to the oxidant menadione and its fluoro analogues acting as effective subversive substrates, the 2-hydroxy-1,4-naphthoquinones lawsone and atovaquone were not observed to inhibit



Scheme 4 Postulated mechanism of CF_3 elimination from trifluoromenadione **3**.

GSSG reduction and to be reduced by the NADPH-reacted enzymes, under the conditions tested. These data suggest that atovaquone and menadione derivatives do not share the same mechanism(s) of action to exert their antimalarial effects.

Finally, CF_3 elimination from the C-3-alkylated trifluoromenadione **5** did not occur through the base-dependent mechanism of lawsone **4** generation from trifluoromenadione **3**. Consequently, a base-catalysed prototropic tautomerism is proposed as the main mechanism to account for the observed CF_3 elimination from trifluoromenadione **3**. These prototropic properties of trifluoromenadione might be exploited in further research to investigate the reaction mechanisms involved in recently described applications based on lawsone as fluorogenic reagent²⁷ or in investigations on atovaquone and lawsone binding sites on human serum albumin.²⁶

Experimental

Chemistry

Melting points were determined on a Büchi melting point apparatus and were not corrected. ^1H (300 MHz), ^{13}C (75 MHz) and ^{19}F (282 MHz) NMR spectra were recorded on a Bruker DRX-300 spectrometer, chemical shifts were expressed in ppm relative to TMS; multiplicity is indicated as s (singlet), d (doublet), t (triplet), q (quadruplet) and m (multiplet). ^{19}F -NMR was performed using 1,2-difluorobenzene as external standard ($\delta = -139.0$ ppm). Elemental analyses were carried out at the Mikroanalytisches Laboratorium der Chemischen Institute der

Universität Heidelberg. ESI MS analyses of the glutathione adducts were performed at the Biochemie-Zentrum (BZH) in the department of Dr J. Lechner. EI MS were recorded at facilities of the Institut für Organische Chemie der Universität Heidelberg. IR spectra were obtained for thin films on KBr-plates on a Bruker Vector 22 FT-IR spectrophotometer. Analytical TLC was carried out on pre-coated Sil G-25 UV_{254} plates from Macherey Nagel. Flash chromatography was performed using silica gel G60 (230–400 mesh) from Macherey Nagel. Starting materials 1,4-dimethoxy-naphthalene **10**,^{5b} 2-bromo-1,4-dimethoxy-naphthalene **11**,²⁸ and 2-*tert*-butyl-1,4-naphthoquinone **15**,²⁹ were synthesized according to reported procedures. The 2-monofluoromenadione **6**, and 2-difluoromenadione **7**, which were previously synthesized as intermediates for further chemistry,^{7,10} were used in our studies.

1,4-Dimethoxy-2-(trifluoromethyl)naphthalene **12**

The reaction was conducted under nitrogen in a three-neck flask with a Dean–Stark apparatus and a thermometer for inside temperature control. To a solution of 2-bromo-1,4-dimethoxy-naphthalene **11** (1.5 g, 5.62 mmol) in 50 mL toluene was added sodium trifluoroacetate (2.29 g, 16.8 mmol) and copper(I) iodide (2.14 g, 11.2 mmol). After addition of 30 mL *N,N*-dimethylacetamide (DMA) the mixture was heated to reflux and the azeotropic water–toluene phase was discarded from the Dean–Stark apparatus. Lost toluene was replaced several times with dry toluene and finally it was distilled out from the reaction mixture until the inside temperature reached $\sim 145^\circ\text{C}$. After 12 h at the

same temperature the solvent was evaporated under reduced pressure and the residue was taken up in 1 vol. CH_2Cl_2 . Mixing with 3 vol. of petroleum ether led to the precipitation of solved copper species and the precipitate was filtered over a small layer of silica gel. The filter cake was washed with petroleum ether– CH_2Cl_2 (2 : 1). The solvent mixture was evaporated and the residual DMA was removed *in vacuo*. The crude mixture was purified over silica gel with petroleum ether– CH_2Cl_2 (3 : 1) as solvent to afford **12** (704 mg, 2.75 mmol, 49% yield) as a white solid. mp 45 °C; δ_{H} (300 MHz; CDCl_3 ; Me_4Si) 8.24–8.29 (1H, m), 8.09–8.13 (1H, m), 7.54–7.63 (2H, m), 6.85 (1H, s), 4.0 (6H) ppm; δ_{C} (75 MHz; CDCl_3 ; Me_4Si) 151.7, 148.9, 128.5, 128.0, 127.3, 127.0, 123.9 (q, $J_{\text{C-F}} = 272.7$ Hz, CF_3), 122.7, 122.3, 118.5 (q, $J_{\text{C-F}} = 30.5$ Hz, C-CF_3), 99.5 (q, $J_{\text{C-F}} = 4.7$ Hz, CH-C-CF_3), 63.5, 55.6 ppm; δ_{F} (282 MHz; CDCl_3 ; 1,2-difluorobenzene) –60.63 ppm. EI MS (70 eV) m/z : 256 ($[\text{M}]^+$, 90%), 241 (100). IR (KBr): $\nu_{\text{max}}/\text{cm}^{-1}$ 3079, 2971, 2994, 2848, 1622, 1590, 1352, 1293, 1226, 1099, 1007. Elemental analysis ($\text{C}_{13}\text{H}_{11}\text{F}_3\text{O}_2$): calc.: C, 60.94; H, 4.33. Found: C, 60.68; H, 4.39.

2-(Trifluoromethyl)naphthalene-1,4-dione **3**

2-Trifluoromethyl-1,4-dimethoxy-naphthalene **12** (600 mg, 2.34 mmol) was dissolved in 10 mL CH_3CN and a CAN solution (3.85 g, 7.02 mmol) in 8 mL H_2O was added. After incubation at room temperature for 20 min, the reaction mixture was poured into water and the aqueous phase was extracted with CH_2Cl_2 and dried over MgSO_4 . The crude mixture was purified over silica gel using petroleum ether– CH_2Cl_2 (3 : 2) to afford **3** (492 mg, 2.17 mmol, 93% yield) as a yellow solid. mp: 103.0 °C, CH_2Cl_2 (lit.³⁰ 104.3 °C, ethanol); δ_{H} (300 MHz; CDCl_3 ; Me_4Si) 8.13–8.19 (1H, m), 8.07–8.13 (1H, m), 7.78–7.87 (2H, m), 7.29 (1H, s) ppm; δ_{C} (75 MHz; CDCl_3 ; Me_4Si) 183.3, 179.4, 136.6 (q, $J_{\text{C-F}} = 4.7$ Hz, CH-C-CF_3), 136.5 (q, $J_{\text{C-F}} = 26.0$ Hz, C-CF_3), 134.6, 134.4, 131.4, 131.3, 126.8, 126.4, 120.6 (q, $J_{\text{C-F}} = 275.2$ Hz, CF_3) ppm; δ_{F} (282 MHz; CDCl_3 ; 1,2-difluorobenzene) –66.24 ppm. EI MS (70 eV) m/z : 226.0 ($[\text{M}]^+$, 100%). IR (KBr): $\nu_{\text{max}}/\text{cm}^{-1}$ 3349, 3101, 3043, 2960, 1672, 1593, 1372, 1282, 1112. Elemental analysis: Found C, 58.57; H, 2.53. Calc. for $\text{C}_{11}\text{H}_5\text{F}_3\text{O}_2$: C, 58.42; H, 2.23.

General procedure for the silver-catalyzed coupling reactions between 1,4-naphthoquinones and carboxylic acids

A solution of a 1,4-naphthoquinone (menadione **2** or trifluoromenadione **3**) (5.81 mmol) and (\pm)-*trans*-4-(4-chlorophenyl)-cyclohexane carboxylic (11.58 mmol) in 52.5 mL acetonitrile was diluted with 17.5 mL water. The mixture was heated to 85 °C. AgNO_3 (90 mg, 0.58 mmol) was added. Then, a solution of $(\text{NH}_4)_2\text{S}_2\text{O}_8$ (1.72 g, 7.54 mmol) in 15 mL acetonitrile and 5 mL water was added dropwise over a period of 45 min. The reaction mixture was heated at reflux for 2 h. The acetonitrile was then removed *in vacuo*, and the aqueous phase was extracted with dichloromethane (4 × 10 mL), dried over MgSO_4 and purified by flash-chromatography.

(\pm)-*trans*-2-[4-(4-Chloro-phenyl)-cyclohexyl]-3-methyl-[1,4]-naphthoquinone **8**

The synthesis of **8** was performed as described above from menadione **2**. After chromatography on silica gel (CH_2Cl_2 –petroleum ether = 3 : 1, UV) and recrystallization from CH_2Cl_2 , **8** (236 mg, 0.65 mmol, 15% yield) was isolated as yellow solid. mp. 99–100 °C (from CH_2Cl_2). δ_{H} (300 MHz; CDCl_3 ; Me_4Si) 7.97–8.01 (m, 2H), 7.57–7.65 (m, 2H), 7.21 (d, $J = 8.4$ Hz, 2H), 7.11 (d, $J = 8.4$ Hz, 2H), 2.88 (tt, $J = 12.1$ Hz, $J = 3.4$ Hz, 1H), 2.62 (tt, $J = 12.2$ Hz, $J = 3.2$ Hz, 1H), 2.18–2.29 (m, 2H), 2.20 (s, 3H), 1.94 (dd, $J = 13.5$ Hz, $J = 2.8$ Hz, 2H), 1.69 (dd, $J = 13.3$ Hz, $J = 3.0$ Hz, 2H), 1.47 (dq, $J = 12.9$ Hz, $J = 3.4$ Hz, 2H) ppm; δ_{C} (75 MHz; CDCl_3 ; Me_4Si) 185.5, 185.1, 150.0, 145.8, 143.4, 133.4, 133.2, 132.8, 131.8, 131.6, 128.5, 128.2, 126.2, 126.1, 43.2, 40.3, 34.56, 30.6, 29.9, 24.8, 12.6 ppm. EI MS (70 eV) m/z : 364 ($[\text{M}]^+$, 100%), 200 (75), 177 (30). IR (KBr): $\nu_{\text{max}}/\text{cm}^{-1}$ 3437, 2923, 2859, 1693, 1658, 1595, 1491, 1450, 1325, 1290, 1259, 1183, 1091, 1010, 1000, 923, 823, 787, 714, 691. Elemental analysis: Found C, 75.43; H, 5.85; Cl, 10.00. Calc. for $\text{C}_{23}\text{H}_{21}\text{ClO}_2$: C, 75.71; H, 5.80; Cl, 9.72.

(\pm)-*trans*-2-[4-(4-Chloro-phenyl)-cyclohexyl]-3-trifluoromethyl-[1,4]naphthoquinone **5**

The synthesis of **5** was performed as described above from **3**. After chromatography on silica gel (CH_2Cl_2 –petroleum ether = 1 : 2, UV), and recrystallization from CH_2Cl_2 , **5** (198 mg, 0.47 mmol, 28% yield) was isolated as yellow solid. mp. 102–104 °C (from CH_2Cl_2). δ_{H} (300 MHz; CDCl_3 ; Me_4Si) 8.03–8.08 (m, 2H), 7.72–7.79 (m, 2H), 7.26 (d, $J = 8.4$ Hz, 2H), 7.16 (d, $J = 8.4$ Hz, 2H), 3.11 (tt, $J = 11.9$ Hz, $J = 3.2$ Hz, 1H), 2.69 (tt, $J = 12.2$ Hz, $J = 3.2$ Hz, 1H), 2.32 (dq, $J = 12.5$ Hz, $J = 3.2$ Hz, 2H), 2.00 (dd, $J = 13.5$ Hz, $J = 2.8$ Hz, 2H), 1.82 (dd, $J = 13.0$ Hz, $J = 2.6$ Hz, 2H), 1.49–1.58 (m, 2H) ppm. δ_{C} (75 MHz; CDCl_3 ; Me_4Si) 184.4, 180.7, 157.1 (q, $J_{\text{C-F}} = 1.1$ Hz, C-C(O)-C-CF_3), 145.4, 134.4, 134.1, 128.5, 128.1, 126.6, 126.4, 122.3 (q, $J_{\text{C-F}} = 280.0$ Hz, CF_3), 43.0, 41.5 (q, $J_{\text{C-F}} = 3.2$ Hz, CH-C-CF_3), 34.2, 30.5, 30.29, 25.57 ppm. EI MS (70 eV) m/z : 418 ($[\text{M}]^+$, 71%), 293 (29), 254 (100), 177 (58), 125 (33). IR (KBr): $\nu_{\text{max}}/\text{cm}^{-1}$ 3463, 2926, 2870, 1674, 1636, 1593, 1581, 1492, 1346, 1286, 1276, 1221, 1173, 1140, 1092, 943, 853, 722, 589. Elemental analysis: Found C, 66.11; H, 4.46; Cl, 8.55. Calc. for $\text{C}_{23}\text{H}_{18}\text{ClF}_3\text{O}_2$: C, 65.96; H, 4.33; Cl, 8.46.

Cyclic voltammetry

Cyclic voltammetry measurements were carried out at 20 °C using platinum working and auxiliary electrodes (CTV 101T and platinum wire, respectively) and a potentiostat (VoltaLab Radiometer Analytical with PGZ 301). The standard calomel reference electrodes were separated from the bulk of the solution by a KCl saturated solution with a glass frit. The compounds (1 mM) were analyzed in CH_2Cl_2 solvent using tetrabutylammonium tetrafluoroborate salt (0.1 M) as supporting electrolyte. Prior to the measurements the mixtures were deoxygenated by means of a stream of dry nitrogen which was maintained above the solutions during measurements. The sweep rate was 0.2 V s^{-1} . I_{pc} and I_{pa} values are respectively the current intensities (μA) for

cathodic and anodic peaks. The standard redox potentials (E°) were determined from cyclic voltammograms by averaging the cathodic (E_{pc}) and the anodic (E_{pa}) peak potentials. The separation of these peak potentials (ΔE_p) can be used to estimate the kinetic reversibility of the respective redox reaction. Menadione **2** and methylene blue (MB) were used as reference compounds. The results are given with reference to the Standard Calomel Electrode (SCE) potential.

Enzymatic studies

Recombinant human and *Plasmodium falciparum* glutathione reductases (GR, E.C.1.8.1.7) were purified as previously reported.^{19,31} One unit of GR activity is defined as the consumption of 1 μ mol NADPH per min ($\epsilon_{340\text{ nm}} = 6.22\text{ mM}^{-1}\text{ cm}^{-1}$) under conditions of substrate saturation. The enzyme stock solutions used for kinetic determinations were >98% pure as judged from silver stained SDS-PAGE. All other reagents were of the highest available purity and were purchased from Biomol, Boehringer, and Sigma.

Glutathione disulfide reduction assays. The standard assay was conducted at 25 °C in a 1 mL-cuvette. The assay mixture contained 100 μ M NADPH and 1 mM GSSG in GR buffer (100 mM potassium phosphate buffer, 200 mM KCl, 1 mM EDTA, pH 6.9). IC_{50} values were evaluated in duplicate in the presence of seven inhibitor concentrations ranging from 0 to 100 μ M. Inhibitor stock solutions were prepared in 100% DMSO. 1% DMSO concentration was kept constant in the assay cuvette. The reaction was started by adding the enzyme (8 mU *h*GR, 6.5 mU *Pf*GR) and the initial rates of NADPH oxidation were monitored at 340 nm ($\epsilon_{340\text{ nm}} = 6.22\text{ mM}^{-1}\text{ cm}^{-1}$). The inhibition of GSSG reduction by **3** was measured as a function of substrate concentration, and the data were fitted by using non-linear regression analysis software (Kaleidagraph) to the equation for non-competitive inhibition.

1,4-Naphthoquinone reductase activity of glutathione reductase. The reduction assay mixture consisted of 100 mM potassium phosphate buffer pH 6.9, 200 mM KCl, 1 mM EDTA and 100 μ M NADPH in a total volume of 1 mL. Fluoromethyl menadione reductase activity was determined by recording the initial velocities in the presence of increasing analogue concentrations (0–300 μ M). The analogues were first dissolved in DMSO, and a final 1% DMSO concentration was kept constant in the 1,4-naphthoquinone reductase assay. For the determination of K_m and V_{max} values, the steady-state rates were fitted by using nonlinear regression analysis software (Kaleidagraph) to the Michaelis–Menten equation. From these values, the turnover number k_{cat} and the catalytic efficiency k_{cat}/K_m were calculated.

Time-dependent inactivation of glutathione reductases by fluoromethyl analogues of menadione. For determining the rate constants of human GR inactivation, the residual GR activity was monitored over time by following an incubation protocol. All reaction mixtures (final volume of 50 μ L) contained 160 μ M NADPH, varying inhibitor concentrations (0–10 μ M), *h*GR (6.85 pmol), 2% DMSO in GR buffer at 25 °C. At different time points (<10 min) 5 μ L-aliquots of each reaction mixture were removed and the residual activity was measured in the standard

GSSG reduction assay at 25 °C (1 mM GSSG and 100 μ M NADPH). 2% DMSO was used in control assays.

Mass spectrometry analysis of fluoro-reacted GR proteins

Samples were prepared in the following way: 15.4 μ M *Pf*GR in 500 μ L GR-buffer was mixed with 200 μ M NADPH and either 200 μ M **3**, or 200 μ M **7** or DMSO alone (control), respectively. At each 60 min period, at room temperature, additional NADPH was added and the solution was again incubated for 60 min (four times). Residual activities of each sample were determined in the 1 mM GSSG reduction assay. Samples were used without further dialysis for mass-spectrometry experiments. Each sample passed through an HPLC column before entering the mass spectrometer by injection on an HPLC system (Agilent 1100 series) coupled on-line to the ESI-QTOF instrument (API QSTAR pulsar PE SCIEX). The protein solution was loaded on a 50 POROS R1 trapping column. After 1.5 min (50% CH_3CN , 40% isopropanol, 0.05% TFA), the proteins were eluted to the electrospray ion source with 90% CH_3CN , 0.05% TFA. The QTOF MS was calibrated by injecting 100 μ L of 1 μ M myoglobin in H_2O . Data were analyzed with the analyst QS software.

Time-dependent formation of glutathione–menadione monoadduct derivatives

GSH (20 mM in H_2O , 50 mL) and inhibitor (20 mM in DMSO, 50 mL) were added to a solution of aqueous NH_4HCO_3 (25 mM, 250 mL) and H_2O (650 mL) and incubated at RT (pH ~7). An aliquot was injected into an HPLC apparatus equipped with a nucleodur® C_{18} column to determine the [menadione derivative]: [monoSG adduct] ratio *versus* time (min) at various time intervals. The HPLC analysis was performed on a Hitachi Merck L-4000 apparatus equipped with a UV detector set at 254 nm. HPLC retention times were obtained using the two following conditions: system A 100% eluent A (0.05% TFA in H_2O) for 5 min, a gradient up to 100% B (0.05% TFA in H_2O – CH_3CN (1/4)) within 10 min, 100% B for 5 min, then again a gradient up to 100% A within 5 min at a flow rate of 1.00 mL min^{-1} . In system A, the 1,4-naphthoquinones were eluted with the following retention times: t_R (trifluoromenadione **5**) = 18.72 min, t_R (difluoromenadione **7**) = 18.43 min, t_R (lawsone **4**) = 15.40 min. System B: 100% eluent A (0.05% TFA in H_2O) for 5 min, a gradient up to 100% B (0.05% TFA in H_2O – CH_3CN (1/4)) within 5 min, 100% B for 15 min, then again a gradient up to 100% A within 5 min at a flow rate of 1.25 mL min^{-1} . In system B, the 1,4-naphthoquinones were eluted with the following retention times: t_R (trifluoromenadione **5**) = 26.26 min, t_R (atovaquone **1**) = 20.42 min.

Chemical stability studies with **3** or **5** by LC-MS analysis

A 10 mM stock solution of **3** or **5** was diluted 1/100 in DMSO then 1/10 in ammonium acetate pH 7.0 at 25 °C to obtain a 10 μ M solution in 10% DMSO. A 1 μ L aliquot was immediately injected on a kinetex 1.7 μ C18 100A column (Phenomenex, Le Pecq, France) and eluted with a 50 : 50 ammonium acetate pH 7.0 : CH_3CN buffer coupled to a LC-MS-APCI instrument

(triple quadrupole mass spectrometer LCMS 8030 Shimadzu). Further injections were performed after 0.5, 1.75, 3.5 and 5 h of incubation. Each experiment was done in duplicate. The trifluoromenadione **3** and the lawsone **4** were analyzed by negative APCI-MS and detected by m/z peaks at 226 and 173 with t_R of 0.4 and 0.15 min, respectively. Known concentrations of trifluoromenadione **3** and lawsone **4** solutions were used for the calibration curves.

In vitro parasite cultures, antiparasitic and cytotoxicity bioassays

The CQ-sensitive 3D7 and the multi-resistant K1 and Dd2 strains of *Plasmodium falciparum* were cultivated using standard protocols previously reported.^{5b,7}

Determination of ED₅₀ values against *P. falciparum* strains.

Drug susceptibility of *P. falciparum* was studied using a modified method³² of the protocol described previously for the ³H-hypoxanthine incorporation-based assay.³³ All assays included CQ diphosphate (Sigma, UK) as standard and control wells with untreated infected and uninfected erythrocytes. ED₅₀ values were derived by sigmoidal regression analysis (Microsoft xfitTM). All data from *in vitro* tests were carried out in triplicate and were given with the 95% confidence limits

Evaluation of cytotoxicity of the different drugs against human KB cell line. Cytotoxicity on human KB cells (human oral pharyngeal carcinoma) was evaluated using the resazurin (Alamar Blue) assay as previously described.⁷

Acknowledgements

The authors are very thankful to Johannes Melcher, BZH and Thomas Ruppert, ZMBH from Heidelberg University for ESI-MS analysis of fluoro-reacted GR proteins. This work has been funded in part by the collaborative center SFB544 (B14 project) and the International Center for Frontier Research in Chemistry icFRC in Strasbourg (www.icfrc.fr). The LC-MS analyses were performed at the TechMed^{ILL} Platform of the Unité Mixte de Service CNRS-Université de Strasbourg (UMS 3286); the authors are grateful to Patrick Gizzi for the data and the fruitful discussions. The authors are indebted to Elena Cesar Rodo for recording the IR spectra of the revised manuscript.

Notes and references

- 1 S. Looareesuwan, C. Viravan, H. K. Webster, D. E. Kyle, D. B. Hutchinson and C. J. Canfield, *Am. J. Trop. Med. Hyg.*, 1996, **54**, 62.
- 2 C. O'Brien, P. P. Henrich, N. Passi and D. A. Fidock, *Curr. Opin. Infect. Dis.*, 2011, **24**, 570.
- 3 M. Fry and M. Pudney, *Biochem. Pharmacol.*, 1992, **43**, 1545.
- 4 (a) A. L. Hopkins, *Nat. Chem. Biol.*, 2008, **4**, 682; (b) G. Bottegoni, A. D. Favia, M. Recanatini and A. Cavalli, *Drug Discovery Today*, 2012, **17**, 23.
- 5 (a) E. Davioud-Charvet, S. Delarue, C. Biot, B. Schwöbel, C. C. Böhme, A. Müssigbrodt, L. Maes, C. Sergheraert, P. Grellier, R. H. Schirmer and K. Becker, *J. Med. Chem.*, 2001, **44**, 4268; (b) W. Friebohn, B. Jannack, N. Wenzel, J. Furrer, T. Oeser, C. P. Sanchez, M. Lanzer, V. Yardley, K. Becker and E. Davioud-Charvet, *J. Med. Chem.*, 2008, **51**, 1260; (c) N. I. Wenzel, N. Chavain, Y. Wang, W. Friebohn, L. Maes, B. Pradines, M. Lanzer, V. Yardley, R. Brun, C. Herold-Mende, C. Biot, K. Tóth and E. Davioud-Charvet, *J. Med. Chem.*, 2010, **53**, 3214; (e) O. Dechy-Cabaret, F. Benoit-Vical, A. Robert and B. Meunier, *ChemBioChem*, 2000, **1**, 281; (e) O. Dechy-Cabaret, F. Benoit-Vical, C. Loup, A. Robert, H. Gornitzka, A. Bonhoure, H. Vial, J. F. Magnaval, J. P. Séguéla and B. Meunier, *Chem.-Eur. J.*, 2004, **10**, 1625; (f) S. A. Laurent, C. Loup, S. Mourgues, A. Robert and B. Meunier, *ChemBioChem*, 2005, **6**, 653; (g) F. Benoit-Vical, J. Lelièvre, A. Berry, C. Deymier, O. Dechy-Cabaret, J. Cazelles, C. Loup, A. Robert, J. F. Magnaval and B. Meunier, *Antimicrob. Agents Chemother.*, 2007, **51**, 1463; (h) B. Meunier, *Acc. Chem. Res.*, 2008, **41**, 69; (i) F. Grellepois, P. Grellier, D. Bonnet-Delpon and J.-P. Bégue, *ChemBioChem*, 2005, **6**, 648; (j) P. M. O'Neill, P. A. Stocks, M. D. Pugh, N. C. Araujo, E. E. Korshin, J. F. Bickley, S. A. Ward, P. G. Bray, E. Pasini, J. Davies, E. Verissimo and M. D. Bachi, *Angew. Chem., Int. Ed.*, 2004, **43**, 4193; (k) S. S. Mahajan, E. Deu, E. M. W. Lauterwasser, M. J. Leyva, J. A. Ellman, M. Bogoyo and A. R. Renslo, *ChemMedChem*, 2011, **6**, 415.
- 6 A. Cavalli and M. L. Bolognesi, *J. Med. Chem.*, 2009, **52**, 7339.
- 7 T. Müller, L. Johann, B. Jannack, M. Brückner, D. A. Lanfranchi, H. Bauer, C. Sanchez, V. Yardley, C. Deregnaucourt, J. Schrével, M. Lanzer, R. H. Schirmer and E. Davioud-Charvet, *J. Am. Chem. Soc.*, 2011, **133**, 11557.
- 8 R. L. Krauth-Siegel, H. Bauer and R. H. Schirmer, *Angew. Chem., Int. Ed.*, 2005, **44**, 690.
- 9 G. Magueur, B. Crousse, S. Charneau, P. Grellier, J.-P. Bégue and D. Bonnet-Delpon, *J. Med. Chem.*, 2004, **47**, 2694.
- 10 H. Bauer, K. Fritz-Wolf, A. Winzer, S. Kühner, S. Little, V. Yardley, H. Vezin, B. Palfey, H. Schirmer and E. Davioud-Charvet, *J. Am. Chem. Soc.*, 2006, **128**, 10784.
- 11 S. Hünig, R. Bau, M. Kemmer, H. Meixner, T. Metzenthin, K. Peters, K. Sinzger and J. Gulbis, *Eur. J. Org. Chem.*, 1998, 335.
- 12 N. Van Tuyen, B. Kesteleyn and N. De Kimpe, *Tetrahedron*, 2002, **58**, 121.
- 13 J. K. Kochi and J. M. Anderson, *J. Am. Chem. Soc.*, 1970, **92**, 1651.
- 14 J. Scheuring, M. Cushman and A. Becher, *J. Org. Chem.*, 1995, **60**, 243.
- 15 T. Gerfaud, H.-L. Wei, L. Neuville and J. Zhu, *Org. Lett.*, 2011, **13**, 6172.
- 16 D. C. Thompson, K. Perera and R. London, *Chem.-Biol. Interact.*, 2000, **126**, 1.
- 17 J. J. Kessl, B. B. Lange, T. Merbitz-Zahradnik, K. Zwickers, P. Hill, B. Meunier, H. Palsdottir, C. Hunte, S. Meshnick and B. L. Trumpower, *J. Biol. Chem.*, 2003, **278**, 31312.
- 18 (a) A. Aumüller and S. Hünig, *Angew. Chem.*, 1984, **96**, 437; (b) A. Aumüller and S. Hünig, *Angew. Chem., Int. Ed. Engl.*, 1984, **23**, 447; (c) A. Aumüller and S. Hünig, *Liebigs Ann. Chem.*, 1986, **1**, 142.
- 19 P. M. Färber, L. D. Arscott, C. H. Williams Jr, K. Becker and R. H. Schirmer, *FEBS Lett.*, 1998, **422**, 311.
- 20 (a) C. Biot, H. Bauer, R. H. Schirmer and E. Davioud-Charvet, *J. Med. Chem.*, 2004, **47**, 5972; (b) K. Buchholz, R. H. Schirmer, J. K. Eubel, M. B. Akoachere, T. Dandekar, K. Becker and S. Gromer, *Antimicrob. Agents Chemother.*, 2008, **52**, 183; (c) C. Morin, T. Besset, J.-C. Moutet, M. Fayolle, M. Brückner, D. Limosin, K. Becker and E. Davioud-Charvet, *Org. Biomol. Chem.*, 2008, **6**, 2731.
- 21 R. Kitz and I. B. Wilson, *J. Biol. Chem.*, 1962, **237**, 3245.
- 22 A. Bellelli, E. Davioud-Charvet, unpublished results.
- 23 H. Amii and K. Uneyama, *Chem. Rev.*, 2009, **109**, 2119.
- 24 E. Davioud-Charvet, D. A. Lanfranchi, Apicomplexan parasites molecular approaches toward targeted drug development, in *Drug Discovery in Infectious Diseases*, ed. K. Becker, P. M. Selzer, Wiley-VCH, Weinheim, 2011, vol. 2.
- 25 W. J. Nickerson, G. Falcone and G. Strauss, *Biochemistry*, 1963, **2**, 537.
- 26 F. Zsila and I. Fitos, *Org. Biomol. Chem.*, 2010, **8**, 4905.
- 27 R. Jelly, S. W. Lewis, C. Lennard, K. F. Lim and J. Almog, *Chem. Commun.*, 2008, 3513.
- 28 K. Karichiappan and D. Wege, *Aust. J. Chem.*, 2000, **53**, 743.
- 29 C. Commandeur, C. Chalumeau, J. Dessolin and M. Laguerre, *Eur. J. Org. Chem.*, 2007, 3045.
- 30 A. F. Helin, A. Veinbjörnsson and C. A. VanderWerf, *J. Am. Chem. Soc.*, 1951, **73**, 1189.
- 31 A. Nordhoff, U. S. Bucheler, D. Werner and R. H. Schirmer, *Biochemistry*, 1993, **32**, 4060.
- 32 A. Cameron, J. Read, R. Tranter, V. J. Winter, R. B. Sessions, R. L. Brady, L. Vivas, A. Easton, H. Kendrick, S. L. Croft, D. Barros, J. L. Lavandera, J. J. Martin, F. Risco, S. Garcia-Ochoa, F. J. Gamo, L. Sanz, L. Leon, J. R. Juiz, R. Gabarro, A. Mallo and F. Gomez de las Heras, *J. Biol. Chem.*, 2004, **279**, 31429.
- 33 R. E. Desjardins, C. J. Canfield, J. D. Haynes and J. D. Chulay, *Antimicrob. Agents Chemother.*, 1979, **16**, 710.